

### Reaction Pathways of the Simmons–Smith Reaction

Masaharu Nakamura,\* Atsushi Hirai,† and Eiichi Nakamura\*

Contribution from the Department of Chemistry, The University of Tokyo,  
Hongo, Bunkyo-ku, Tokyo 113-0033, Japan

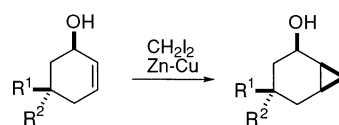
Received April 28, 2002; E-mail: masaharu@chem.s.u-tokyo.ac.jp; nakamura@chem.s.u-tokyo.ac.jp

**Abstract:** The cyclopropanation reaction of an alkene with a metal carbenoid has been studied by means of the B3LYP hybrid density functional method. The cyclopropanation of ethylene with a lithium carbenoid or a zinc carbenoid [Simmons–Smith (SS) reagent] goes through two competing pathways, methylene transfer and carbometalation. Both processes are fast for the lithium carbenoid, while, for the zinc carbenoid, only the former is fast enough to be experimentally feasible. The reaction of an SS reagent (ClZnCH<sub>2</sub>Cl) with ethylene and an allyl alcohol in the presence of ZnCl<sub>2</sub> was also studied. The allyl alcohol reaction was modeled with an SS reagent/alkoxide complex (ClCH<sub>2</sub>ZnOCH<sub>2</sub>CH=CH<sub>2</sub>) formed from the SS reagent and allyl alcohol. Two modes of acceleration were found. The first involves the well-accepted mechanism of 1,2-chlorine migration, and the second involves a five-centered bond alternation. The latter was found to be more facile than the former and to operate equally well both with ethylene and with aggregates of SS reagent/alkoxide complexes. Calculations on the SS reaction with 2-cyclohexen-1-ol offer a reasonable model for the hydroxy-directed diastereoselective SS reaction, which has been used for a long time in organic synthesis.

A reaction between iodomethylzinc iodide and an olefin that produces a cyclopropane compound was first reported by Simmons and Smith in 1958<sup>1</sup> and is now called the Simmons–Smith (SS) reaction. Although iodomethylzinc iodide prepared from CH<sub>2</sub>I<sub>2</sub> and metallic zinc was the original SS reagent, the Furukawa reagent prepared by a halogen–metal exchange reaction between Et<sub>2</sub>Zn and CH<sub>2</sub>I<sub>2</sub><sup>2</sup> is also used widely for synthesis because of its reproducibility. Several zinc carbenoids (XZnCH<sub>2</sub>Y) composed of chloro/iodo and chloro/chloro combinations are as effective as the original iodo/iodo combination (hence, ClZnCH<sub>2</sub>Cl was mainly studied in the present work).<sup>3</sup>

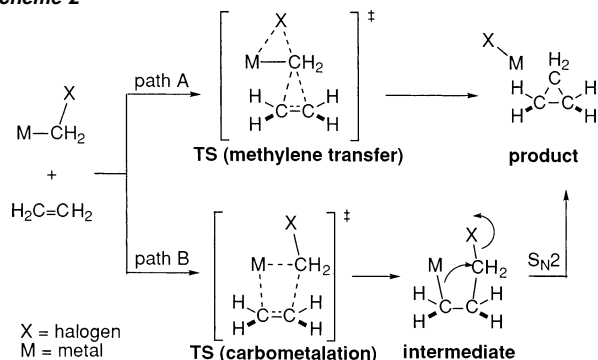
Winstein et al. reported the first application of the SS reaction to an allylic alcohol in 1959,<sup>4</sup> which represents an early example of the use of a heteroatom group as a “directing group”. The SS reaction with an allylic alcohol has distinct advantages over the reaction with a simple olefin in relation to the reaction rate and stereocontrol. Rickborn reported that the SS reactions of allylic alcohols are much faster than those of simple olefins (ca. >1000 times) and that the reaction with a cyclic allylic alcohol takes place in such a manner that the cyclopropane ring forms on the same side as the hydroxyl group (Scheme 1).<sup>5</sup> The SS reaction with *cis*-5-methyl-2-cyclohexen-1-ol was 3.35

Scheme 1



entry	R <sup>1</sup>	R <sup>2</sup>	k <sub>rel</sub>
1	H	Me	1.00
2	H	H	2.17
3	Me	H	3.35

Scheme 2



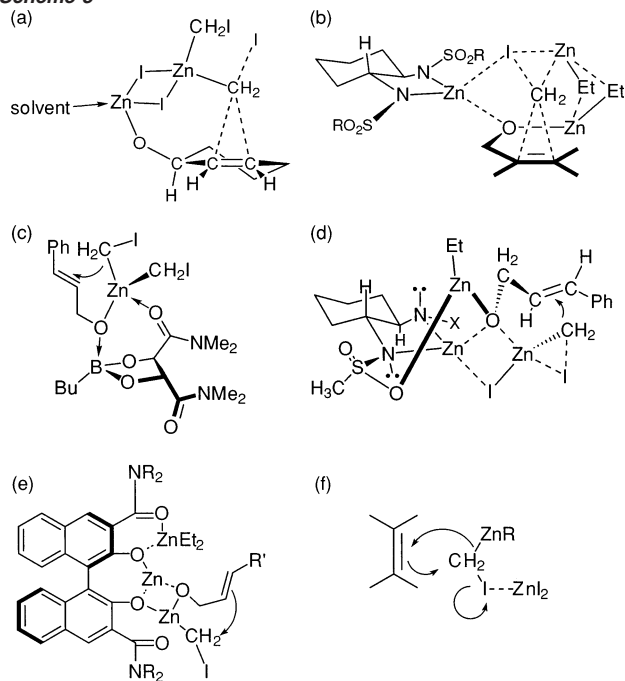
times faster than that with the corresponding *trans*-alcohol (entries 3 and 1 in Scheme 1). The rate constant of the cyclopropanation with 2-cyclohexen-1-ol lies between those of *cis*- and *trans*-5-methyl-2-cyclohexen-1-ols (entry 2).

Numerous variants of the SS reagents have been explored in organic syntheses, but little is known about their reaction pathways. Earlier mechanistic controversy focused on the dichotomy between a methylene transfer mechanism and a carbometalation mechanism (Scheme 2). It was originally suggested that the SS reaction occurs by a one-step methylene transfer mechanism, in which the pseudotrigonal methylene group of iodomethylzinc iodide adds to an olefin  $\pi$ -bond and

† Present address: Division of Chemistry, Graduate School of Science, Hokkaido University, 060-0810 Sapporo, Japan.

- (1) Simmons, H. E.; Smith, R. D. *J. Am. Chem. Soc.* **1958**, *80*, 5323–5324.
- (2) Furukawa, J.; Kawabata, N.; Nishimura, J. *Tetrahedron Lett.* **1966**, *7*, 3353–3355.
- (3) (a) Denmark, S. E.; Edwards, J. P. *J. Org. Chem.* **1991**, *56*, 6974–6981. (b) Denmark, S. E.; Edwards, J. P.; Wilson, S. R. *J. Am. Chem. Soc.* **1992**, *114*, 2592–2602.
- (4) (a) Winstein, S.; Sonnenberg, J.; de Vries, L. *J. Am. Chem. Soc.* **1959**, *81*, 6523–6524. (b) Winstein, S.; Sonnenberg, J. *J. Am. Chem. Soc.* **1961**, *83*, 3235–3244.
- (5) (a) Chan, J. H.-H.; Rickborn, B. *J. Am. Chem. Soc.* **1968**, *90*, 6406–6411. (b) Staroscik, J. A.; Rickborn, B. *J. Org. Chem.* **1972**, *37*, 738–740.

Scheme 3



forms two new C–C bonds simultaneously, accompanying a 1,2-migration of the halide anion from the carbon atom to the zinc atom (path A in Scheme 2). There is experimental evidence for the SS reagent that contradicts with path B, and thus path A has been widely believed to represent the experimental reality. For lithium carbenoids, on the other hand, the alternative carbometalation/cyclization pathway has received experimental support.<sup>6</sup> The study of the factors that determine the reaction pathways of metal carbenoid addition to olefins is, therefore, still in question.<sup>7</sup>

More recent discussions have focused on the role of Lewis acids, especially chiral Lewis acids. Various working models reported in the literature are summarized in Scheme 3. One model proposed by Wittig<sup>8,9</sup> assumes that  $ZnI_2$  coordinates the leaving iodine atom, and all others assume that either the leaving iodine atom undergoes 1,2-migration to the neighboring zinc atom (i.e., b and d; path A in Scheme 2) or it leaves simply by itself (a and e). The Wittig proposal has thus far received little attention, and the great majority of the literature and textbooks assume the 1,2-halide migration. Perhaps the most significant lack of common understanding is the fundamental reactivity of the SS reagent, as implied by the existence of three schools of arrow formalisms, drawing an arrow from carbene to the olefin (Scheme 3c and d), an arrow from the olefin to the carbene carbon (e), or two arrows simultaneously (f).<sup>8,10</sup>

- (6) Stiasny, H. C.; Hoffmann, R. W. *Chem.-Eur. J.* **1995**, *1*, 619–624.  
 (7) For a review of the structure and reactivity of metal carbenoids and their analogues: Boche, G.; Lohrenz, J. C. W. *Chem. Rev.* **2001**, *101*, 697–756.  
 (8) Wittig, G.; Wingler, F. *Chem. Ber.* **1964**, *97*, 2146–2164.  
 (9) Friedrich, E. C.; Lunetta, S. E.; Lewis, E. J. *J. Org. Chem.* **1989**, *54*, 2388–2390.  
 (10) Such a lack of consistency is frequently seen in the literature despite the earlier demonstration of the higher reactivity of electron-rich olefins in the SS reaction. Proposed mechanisms of Lewis acid acceleration: (a) Chan, J. H.-H.; Rickborn, B. *J. Am. Chem. Soc.* **1968**, *90*, 6406–6411. (b) Takahashi, H.; Yoshioka, M.; Ohno, M.; Kobayashi, S. *Tetrahedron Lett.* **1992**, *33*, 2575. (c) Charette, A. B.; Brochu, C. *J. Am. Chem. Soc.* **1994**, *116*, 2651. (d) Kitajima, H.; Ito, K.; Aoki, Y.; Katsuki, K. *Bull. Chem. Soc. Jpn.* **1997**, *70*, 207.

As summarized in the previous paragraph, there has been a paucity of information on the mechanism of the SS reaction, which is due largely to the difficulties in carrying out suitable experimental studies: the SS reagent is unstable under the reaction conditions, making both precise kinetics studies and identification of reactive species difficult. The Cambridge Crystallographic Data Base has four structures related to the SS reagent. A  $\mu$ -chloro-bridged dimer,  $(CF_3CCl_2ZnCl \cdot Et_2O)_2$ ,<sup>11</sup> is a genuine SS reagent, although it is inactive due to the strong electron-withdrawing effects of the many halogen atoms. The other crystal structures of SS-related reagents are those of  $(ClCH_2)_2Zn$  stabilized with a didentate ligand,<sup>12</sup> but it is still unclear as to what extent this structure is relevant to the mechanism of the SS reaction.

We describe the mechanism of the SS reaction examined with the aid of density functional theory focusing on various unsolved issues of the SS reaction, including (1) the methylene transfer/carbometalation dichotomy, (2) Lewis acid acceleration, (3) the allylic alcohol reaction, (4) Lewis acid effects and aggregate formation in the allylic alcohol reaction, and (5) the diastereo-face-directing effect in the reaction of 2-cyclohexen-1-ol.<sup>13</sup> Together with some recent theoretical studies,<sup>14</sup> the present studies provide mechanistic information that is not obtainable by experimental methods.

## Computational Method

Calculations were performed with the Gaussian 94 and Gaussian 98 programs.<sup>15</sup> Most of the calculations were performed using the density functional theory B3LYP method, which is a hybrid functional of the Hartree–Fock and density functional methods,<sup>16</sup> using a split valence basis set with polarization functions for heavy atoms. The B3LYP results were compared with the HF, MP2, and other results when necessary. Ahlrichs' SVP<sup>17</sup> all-electron basis set was used for the zinc atom, and the 6-31G\* or 3-21G\* basis set<sup>18</sup> was used for other atoms (denoted here as B3LYP/631A and B3LYP/321A, respectively). The Hay–Wadt effective core potential (ECP), LANL2DZ, was used for the iodine atom.<sup>19</sup>

Structures were optimized without any geometrical assumption, unless otherwise noted. Zero imaginary frequencies for equilibrium

- (11) Behm, J.; Lotz, S. D.; Herrmann, W. A. *Z. Anorg. Allg. Chem.* **1993**, *619*, 849–852.  
 (12) Denmark, S. E.; Edwards, J. P.; Wilson, S. R. *J. Am. Chem. Soc.* **1991**, *113*, 723–725. Charette, A. B.; Marcoux, J.-F.; Bélanger-Gariépy, F. *J. Am. Chem. Soc.* **1996**, *118*, 6792–6793. Charette, A. B.; Marcoux, J.-F.; Molinaro, C.; Beauchemin, A.; Brochu, C.; Isabel, E. *J. Am. Chem. Soc.* **2000**, *122*, 4508–4509.  
 (13) A part of this paper was described in: (a) Hirai, A.; Nakamura, M.; Nakamura, E. *Chem. Lett.* **1998**, 927–928. (b) Nakamura, E.; Hirai, A.; Nakamura, M. *J. Am. Chem. Soc.* **1998**, *120*, 5844–5845.  
 (14) (a) Comparison between cyclopropanation and  $Csp^2$ -H insertion: (a) Bernardi, F.; Bottini, A.; Miscione, G. P. *J. Am. Chem. Soc.* **1997**, *119*, 12300–12305. (b) A theoretical study on the methylene transfer pathways of cyclopropanation of ethylene with lithium carbenoids and zinc carbenoids was reported recently, and a conclusion essentially the same as ours has been drawn. Hermann, H.; Lohrenz, J. C. W.; Kühn, A.; Boche, G. *Tetrahedron* **2000**, *56*, 4109–4115. (c) DFT (BP and BLYP) calculations on the same system with (relativistic) effective core potentials, (R)ECPs, for iodine and zinc were reported, where the transition structure and activation energy of the SS reaction were essentially the same as those of the present work: Dargel, T. K.; Koch, W. *J. Chem. Soc., Perkin Trans. 2* **1996**, 877. (d) The same model was examined by Fang and Phillips using the B3LYP method with large basis sets (6-311G\*\* or larger). While the activation energy of the SS reaction varies from ca. 10 to 20 kcal/mol depending on the method and basis sets, the structural feature of the transition structure in the present work is in good agreement with that reported in the reference: Fang, W.-H.; Phillips, D. L.; Wang, D.-Q.; Li, Y.-L. *J. Org. Chem.* **2002**, *67*, 154–160. (e) For an earlier Hückel MO study, see: Hida, M. *Bull. Chem. Soc. Jpn.* **1967**, *40*, 2497–2501. (f) A theoretical investigation on the reaction mechanism of the cyclopropanation of olefins with monomeric metal carbenoids, which included  $LiCH_2I$ ,  $IzCH_2I$ , and a variety of iodomethylzinc aryloxide, has been reported by Phillips and Fang: Wang, D.; Phillips, D. L.; Fang, W.-H. *Organometallics* **2002**, *21*, 5901–5910.

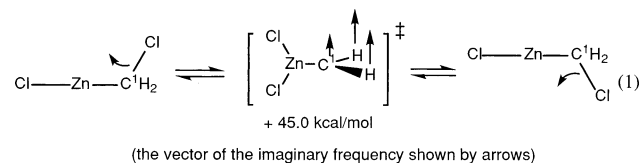
**Table 1.** Activation Energies of the Cyclopropanation Reaction of Ethylene with **5** Obtained by Several Methods

entry	method	$\Delta E^\ddagger$
1	CCSD(T)/6311A//B3LYP/631A	+19.5
2	MP4/631A/B3LYP/631A	+20.0
3	MP2/631A/B3LYP/631A	+21.7
4	B3LYP/631A	+17.3
5	B3LYP/631A/HF/321A	+18.4
6	HF/321A	+6.0

structures and one for transition structures (TSs) were confirmed by the normal coordinate analysis. The intrinsic reaction coordinate (IRC) analyses of some reactions were performed at the B3LYP/631A level.<sup>20</sup> The energies were recalculated at the B3LYP/631A level for the HF/321A geometry (Table 1).<sup>21</sup> Energetics are discussed on the basis of the potential energy. The self-consistent reaction field (SCRF)<sup>22</sup> method (polarized continuum model) was applied to the molecular geometry obtained at the B3LYP/631A level to estimate the effect of the polarity of bulk solvent on the energies.

## Results and Discussion

**1. Methylene Transfer versus Carbometalation.** To start the investigation, we examined the possibility of free carbene formation from the SS reagent. Elongating the C<sup>1</sup>–Cl bond in ClZnCH<sub>2</sub>Cl, we obtained a zinc carbene complex structure as a stationary point (eq 1), which, however, is the transition state for the exchange of the two chlorine atoms. The result indicates that free carbene and zinc-carbene complex intermediates are unlikely reactive intermediates in the SS reaction.



There has been experimental evidence that the SS reaction does not take place via a carbometalation mechanism (path B

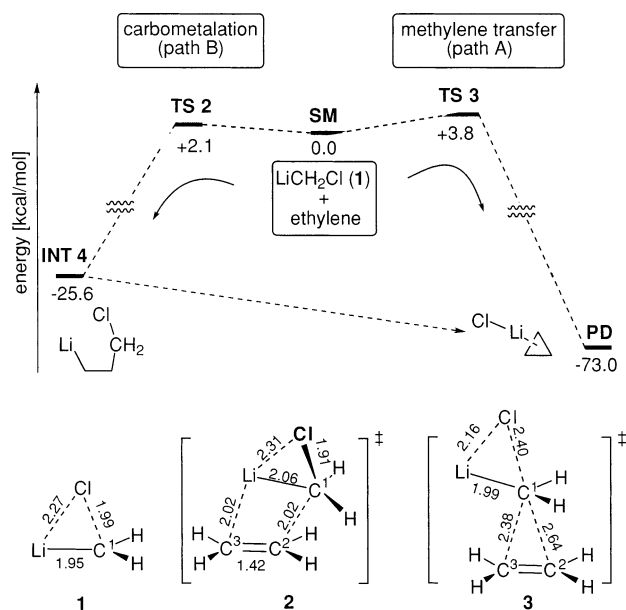


**Figure 1.** Cyclopropanation of ethylene with LiCH<sub>2</sub>Cl (B3LYP/631A level). Bond lengths are given in angstroms, and energies relative to SM are shown in kilocalories per mole. In all figures in this article, starting materials, reactants, reaction intermediates, transition structures, and products are denoted as SM, RT, INT, TS, and PD, respectively.

in Scheme 2),<sup>8</sup> and hence it was concluded that the reaction takes place via a methylene transfer pathway (path A). On the other hand,  $\alpha$ -halomethyl lithium reagents cyclopropanate olefins via both a methylene transfer and a carbometalation/cyclization mechanism depending on slight stereochemical differences in the substrate.<sup>6</sup> The reason for such a metal-dependent dichotomy has remained unclear. To investigate the diversity of the reaction pathways, we compared the cyclopropanation reaction with LiCH<sub>2</sub>Cl (**1**) and ClZnCH<sub>2</sub>Cl (**5**) along the two reaction pathways A and B shown in Figures 1 and 2, respectively.<sup>13,14b</sup> In the methylene transfer pathway (path A in Scheme 2), concerted [2 + 1] addition takes place to provide a cyclopropane ring through the transition structure (TS) **3** or **7**, respectively. On the other hand, in the carbometalation pathway (path B), insertion reaction of an olefin to the metal–carbon bond occurs to produce an intermediate (**4** or **8**, respectively) through the four-centered TS **2** or **6**. A subsequent intramolecular substitution reaction of **4** or **8** produces the cyclopropane product.

The two reaction pathways of the cyclopropanation were examined first for the lithium carbenoid. As shown in the energy diagram (Figure 1), the energy difference between **2** and **3** is very small, the former is higher in energy than the starting material by 2.1 kcal/mol, and the latter is 3.8 kcal/mol higher in energy than the starting material. These data agree with the experimental fact that the two pathways compete with each other

- (15) Frisch, M. J.; Trucks, G. W.; Schlegel, H. B.; Gill, P. M. W.; Johnson, B. G.; Robb, M. A.; Cheeseman, J. R.; Keith, T.; Petersson, G. A.; Montgomery, J. A.; Raghavachari, K.; Al-Laham, M. A.; Zakrzewski, V. G.; Ortiz, J. V.; Foresman, J. B.; Cioslowski, J.; Stefanov, B. B.; Nanayakkara, A.; Challacombe, M.; Peng, C. Y.; Ayala, P. Y.; Chen, W.; Wong, M. W.; Andres, J. L.; Replogle, E. S.; Gomperts, R.; Martin, R. L.; Fox, D. J.; Binkley, J. S.; Defrees, D. J.; Baker, J.; Stewart, J. P.; Head-Gordon, M.; Gonzalez, C.; Pople, J. A. *Gaussian 94*, revision D.1; Gaussian, Inc.: Pittsburgh, PA, 1995. Frisch, M. J.; Trucks, G. W.; Schlegel, H. B.; Scuseria, G. E.; Robb, M. A.; Cheeseman, J. R.; Zakrzewski, V. G.; Montgomery, J. A., Jr.; Stratmann, R. E.; Burant, J. C.; Dapprich, S.; Millam, J. M.; Daniels, A. D.; Kudin, K. N.; Strain, M. C.; Farkas, O.; Tomasi, J.; Barone, V.; Cossi, M.; Cammi, R.; Mennucci, B.; Pomelli, C.; Adamo, C.; Clifford, S.; Ochterski, J.; Petersson, G. A.; Ayala, P. Y.; Cui, Q.; Morokuma, K.; Malick, D. K.; Rabuck, A. D.; Raghavachari, K.; Foresman, J. B.; Cioslowski, J.; Ortiz, J. V.; Baboul, A. G.; Stefanov, B. B.; Liu, G.; Liashenko, A.; Piskorz, P.; Komaromi, I.; Gomperts, R.; Martin, R. L.; Fox, D. J.; Keith, T.; Al-Laham, M. A.; Peng, C. Y.; Nanayakkara, A.; Challacombe, M.; Gill, P. M. W.; Johnson, B.; Chen, W.; Wong, M. W.; Andres, J. L.; Gonzalez, C.; Head-Gordon, M.; Replogle, E. S.; Pople, J. A. *Gaussian 98*, revision A.9; Gaussian, Inc.: Pittsburgh, PA, 1998.
- (16) Stephens, P. J.; Devlin, F. J.; Chabalowski, C. F.; Frisch, M. J. *J. Phys. Chem.* **1994**, *45*, 11623–11627 and references therein.
- (17) Schäfer, A.; Horn, H.; Ahlrichs, R. *J. Chem. Phys.* **1992**, *97*, 2571–2577.
- (18) Split valence basis set (6-31G): Ditchfield, R.; Hehle, W. J.; Pople, J. A. *J. Chem. Phys.* **1971**, *54*, 724–728. Hehre, W. J.; Ditchfield, R.; Pople, J. A. *J. Chem. Phys.* **1972**, *56*, 2257–2261. Polarized basis set: Hariharan, P. C.; Pople, J. A. *Theor. Chim. Acta* **1973**, *28*, 213–222.
- (19) Hay, P. J.; Wadt, W. R. *J. Chem. Phys.* **1985**, *82*, 270–283. Wadt, W. R.; Hay, P. J. *J. Chem. Phys.* **1985**, *82*, 284–298. Hay, P. J.; Wadt, W. R. *J. Chem. Phys.* **1985**, *82*, 299–310.
- (20) (a) Fukui, K. *Acc. Chem. Res.* **1981**, *14*, 363–368. (b) Ishida, K.; Morokuma, K.; Komornicki, A. *J. Chem. Phys.* **1977**, *66*, 2153–2156. (c) Gonzalez, C.; Schlegel, H. B. *J. Chem. Phys.* **1989**, *90*, 2154–2161. (d) Schlegel, H. B.; Gonzalez, C. *J. Phys. Chem.* **1990**, *94*, 5523–5527.
- (21) To confirm the accuracy of the theoretical method, we made a comparison of the activation energies of the cyclopropanation reaction of **5** with ethylene for various methods. As shown in Table 1, B3LYP, MP2, and MP4 energies (for the B3LYP geometry) are similar to that obtained by the coupled cluster method (CCSD(T)) ( $\Delta E^\ddagger = 19.5$  kcal/mol, entry 1) and were judged to be reliable. The geometry obtained by HF/321A (data not shown) is similar to that obtained by the B3LYP method, and the activation energy obtained by a single point calculation at the B3LYP/631A level is similar to that obtained at the CCSD(T)/631A level (entries 5 and 6). The B3LYP/631A//HF/321A data are therefore used for the studies of very large systems (vide infra) with the single point calculation using the B3LYP method (entries 5 and 6).
- (22) (a) Wong, M. W.; Wiberg, K. B.; Frisch, M. J. *J. Chem. Phys.* **1991**, *95*, 8991–8998. (b) Wong, M. W.; Frisch, M.; Wiberg, K. B. *J. Am. Chem. Soc.* **1991**, *113*, 4776–4782.

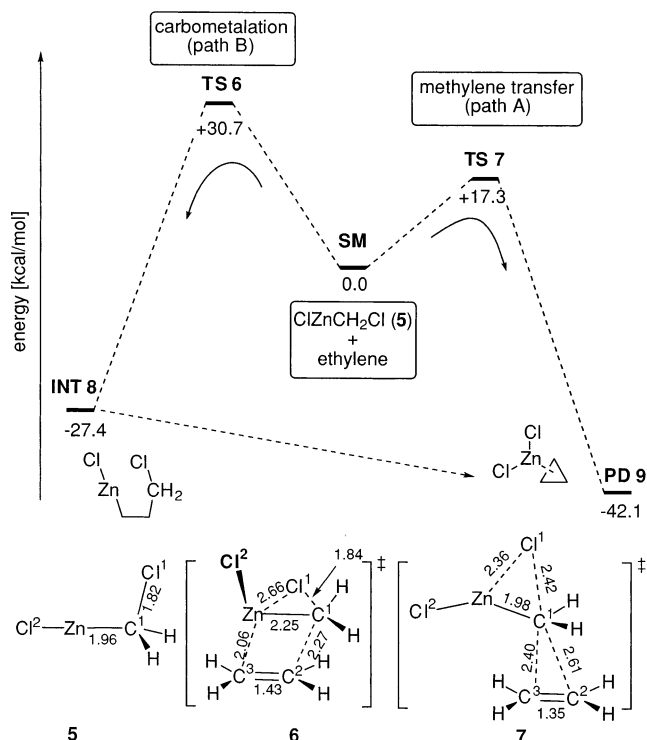


**Figure 2.** Cyclopropanation of ethylene with ClZnCH<sub>2</sub>Cl (B3LYP/631A level). Bond lengths are given in angstroms, and energies relative to SM are shown in kilocalories per mole.

in cyclopropanation reactions with lithium carbenoids.<sup>6</sup> Several points are noteworthy as to the structures of the stationary points. The chlorine atom is already detached from the methylene carbon (C<sup>1</sup>) in the starting chloromethyl lithium (1), and the methylene group is almost sp<sup>2</sup> hybridized (dihedral angle H–C–Li–H = 178.0°, angle Li–C–H = 126.4°, angle H–C–H = 107.2°). The lithium carbenoid can be regarded as a complex between methylene carbene and lithium chloride. The core four-centered part of the TS of carbometalation (2) is similar to that of MeLi addition to ethylene,<sup>23</sup> and the TS of the methylene transfer (3) can be viewed as the transition state of S<sub>N</sub>2 displacement of the chlorine atom by ethylene (note that the Li–C<sup>1</sup> bond is not greatly elongated; see also discussion in Figure 3).

Very different energetics were obtained for the zinc carbenoid: the methylene transfer pathway is overwhelmingly favored over the carbometalation pathway (Figure 2). The TS of the carbometalation pathway (6) is C<sub>1</sub> symmetric, as with 2. Although TS 6 has a structure similar to that of TS 2, the activation energy (30.7 kcal/mol) is much higher than that of the carbolithiation (2.1 kcal/mol). This high activation energy is due to the energy required to cleave the covalent C–Zn bond, which is larger than the energy to achieve bond reorganization in 2 involving the breakage of the ionic C–Li bond. The activation energy of the methylene transfer pathway (7) is much lower (17.3 kcal/mol), which is a reasonable value for the SS reaction that takes place around room temperature.<sup>24</sup> Note that the lithium carbenoid reactions take place at lower temperatures (e.g., –78 °C). The Cl<sup>2</sup>–Zn–C<sup>1</sup> bond that is linear in the starting SS reagent 5 (i.e., favored geometry for a Zn(II) species) is bent in the TS to accommodate the incoming Cl<sup>1</sup> anion, which

(23) Nakamura, M.; Nakamura, E.; Koga, N.; Morokuma, K. *J. Chem. Soc., Faraday Trans.* **1994**, *29*, 1789–1798.

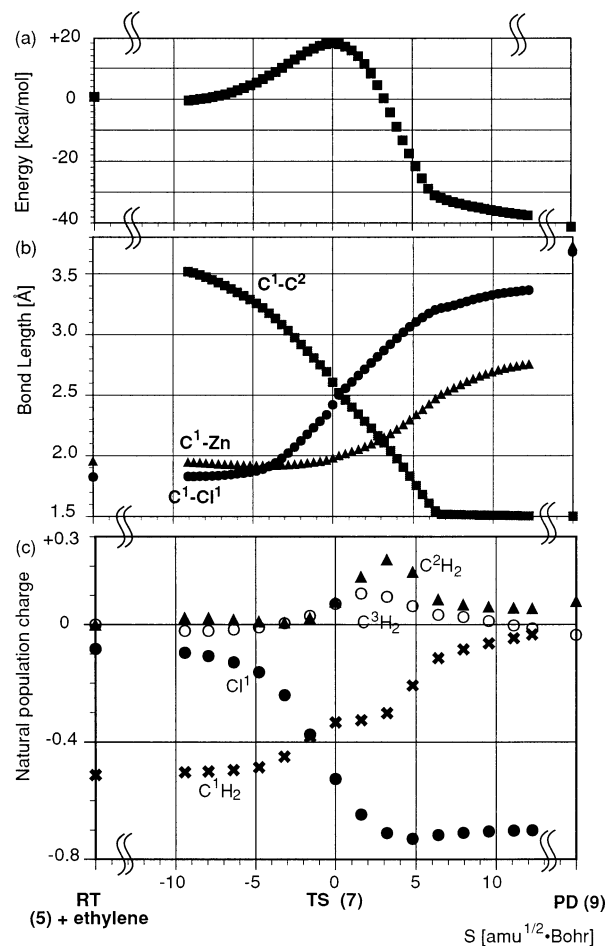


**Figure 3.** The energetics of the SS reaction in Figure 2: (a) energy change, (b) bond length changes, and (c) natural population charge in IRC analysis near 7 at the B3LYP/631A level.

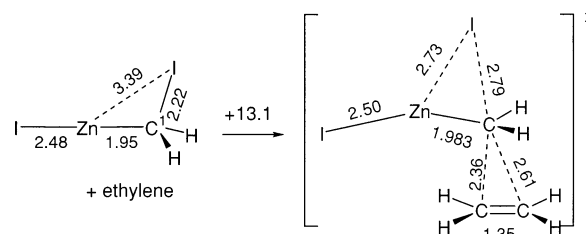
in turn indicates that the leaving-group ability of the Cl<sup>1</sup> is enhanced by association with the zinc atom in the TS. Such a Lewis acid assistance coincides with the prevailing hypothesis of the 1,2-halide migration (vide supra).

The cyclopropanation with iodomethylzinc iodide was also examined at the B3LYP/631A level (see ref 25). The activation energy (13.1 kcal/mol) was found to be ca. 4.2 kcal/mol lower than that of 7, and the geometry of the TS was essentially the same as that of the chlorozinc reagent (Figure 3b).

Analysis of the potential energy surface along the IRC (Figure 3) confirms that the SS reagent (5) and ethylene are connected

(24) The calculated <sup>13</sup>C kinetic isotope effect (KIE) with tunnel correction of the two TSs 6 and 7 is as follows: C<sup>1</sup>, 1.029; C<sup>2</sup>, 1.027; C<sup>3</sup>, 1.071 in 6; C<sup>1</sup>, 1.066; C<sup>2</sup>, 1.003; C<sup>3</sup>, 1.008 in 7 (scale factor of 0.9804: Wong, M. W. *Chem. Phys. Lett.* **1996**, *255*, 391–399. Theory of KIE: Bigeleisen, J. *J. Chem. Phys.* **1949**, *17*, 675–678). The trend in KIEs for 7 differs significantly from that of 6 and hence will serve as experimental evidence to differentiate the reaction pathway.

(25) Cyclopropanation of ethylene with iodomethylzinc iodide at the B3LYP/631A level. The optimized structures as shown below are virtually the same as the structure reported previously.<sup>14c,d</sup>



to the product **9** via **7** without any intermediate. When one looks into the details of Figure 3b, one may note that the C<sup>1</sup>–C<sup>2</sup> bond formation and the C<sup>1</sup>–Cl<sup>1</sup> bond cleavage occur in a concordant manner, but the C<sup>1</sup>–Zn bond cleavage occurs at a later stage of the reaction. The C<sup>1</sup>–Cl<sup>1</sup> bond at TS **7** ( $S = 0$ ) is stretched by as much as 25%, but the C<sup>1</sup>–Zn bond is stretched by only 7% as compared with the respective bonds in the starting material **5**.

The data in Figure 3c (natural population charge) reveal that the reaction takes place in two stages. The first event takes place between the reactants (**5** + ethylene) on the way to TS **7**. The chlorine atom Cl<sup>1</sup> gains negative charge, while the methylene group (C<sup>1</sup>H<sub>2</sub>) and the olefin (C<sup>2</sup>H<sub>2</sub> and C<sup>3</sup>H<sub>2</sub>) lose electrons. This change of charge density as well as the elongation of the C<sup>1</sup>–Cl<sup>1</sup> bond (Figure 3b) around **7** indicate that the key event in the SS reaction is a nucleophilic displacement of the leaving halide group with an olefin. The second event takes place on the way from **7** to the product (around  $S = 5$ ). The electron densities at C<sup>2</sup>H<sub>2</sub> and C<sup>3</sup>H<sub>2</sub> increase again because of the C<sup>1</sup>–Zn bond cleavage that results in the formation of a neutral cyclopropane ring. In summary, the methylene transfer pathway takes place through two stages: an S<sub>N</sub>2-like displacement reaction by ethylene on halomethylzinc, followed by cleavage of the C<sup>1</sup>–Zn bond to give the cyclopropane ring (vide infra).

**2. Lewis Acid Acceleration of the SS Reaction. Cyclopropanation of Ethylene.** Having established the methylene transfer pathway as the dominant mechanism of the SS cyclopropanation reaction, we next investigated how a Lewis acid (LA) might accelerate the reaction. Zinc halide (ZnCl<sub>2</sub>), which forms in situ as a byproduct of the cyclopropanation and is known to accelerate the SS reaction,<sup>26</sup> was used as a model Lewis acid. An ether complex of dimeric 1,1,1-trifluoro-2,2-dichloroethylzinc chloride, (CF<sub>3</sub>CCl<sub>2</sub>ZnCl·Et<sub>2</sub>O)<sub>2</sub>,<sup>11</sup> has a di- $\mu$ -chloro-dizinc(II) four-centered structure and was used to generate structure **10** to act as a model of the ZnCl<sub>2</sub>/SS reagent complex. We also considered its “open” cluster **11**, wherein the “closed” chloride bridge structure in **10** opens to form a five-centered structure (Figure 4). In **11**, ZnCl<sub>2</sub> directly activates the Cl<sup>1</sup> leaving group, and the C<sup>1</sup>–Cl<sup>1</sup> bond is elongated. The open cluster **11** is less stable than **10** (by 3.5 kcal/mol). The energetics of the reaction pathways, modes 1 and 2, are also shown in Figure 4.

In mode 1 activation, **10** (C<sub>s</sub>) reacts with ethylene in a single-step reaction with retention of C<sub>s</sub> symmetry throughout the reaction course along the IRC. The reaction proceeds through **12** to give a product **14** (a complex between a cyclopropane and a zinc chloride dimer) with 44.9 kcal/mol exothermicity. The 1,2-migration of Cl<sup>1</sup> from C<sup>1</sup> to Zn<sup>1</sup> is taking place in **12**. In comparison with the prototypical reaction (ClZnCH<sub>2</sub>Cl + ethylene,  $\Delta E^\ddagger = 17.3$  kcal/mol, B3LYP/631A),  $\Delta E^\ddagger$  in mode 1 is 4.7 kcal/mol lower (12.6 kcal/mol).<sup>27</sup> Coordination of the Lewis acid ZnCl<sub>2</sub> on Zn<sup>1</sup> facilitates the 1,2-chloride migration in the reaction pathway. The C<sup>1</sup>–Cl<sup>1</sup> bond is elongated (32% longer than in **10**), but the C<sup>1</sup>–Zn bond is not cleaved yet (0.9% elongated).

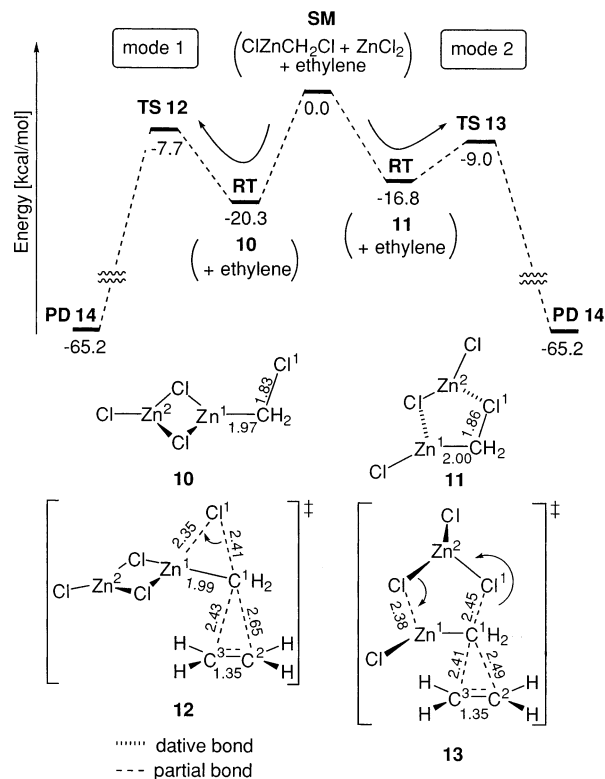


**Figure 4.** Cyclopropanation of ethylene with ClZnCH<sub>2</sub>Cl in the presence of a Lewis acid ZnCl<sub>2</sub> (B3LYP/631A level). Energies relative to the starting materials (SM) are shown in kilocalories per mole. Bond lengths in optimized structures are shown in angstroms.

IRC analysis of the mode 2 pathway reveals that **11**, **13**, and a cyclopropane product are smoothly connected with each other along the IRC. The five-centered complex **11** (C<sub>s</sub>) reacts with ethylene via **13** (C<sub>1</sub>) with 7.8 kcal/mol activation energy (mode 2), which is much lower than that in mode 1 activation. In addition, mode 2 is thermodynamically favored over path A by 1.3 kcal/mol. The Cl<sup>1</sup>–C<sup>1</sup> bond fission takes place in a five-centered manner, and Cl<sup>1</sup> becomes attached to Zn<sup>2</sup> later along the IRC. Ethylene approaches the methylene carbon, and the leaving chlorine atom is moving in the direction opposite to that of ethylene. As shown in the global energy diagram in Figure 4, the SS reagent **11** goes to the cyclopropane product with lower activation barrier than does the isomer **10**. This is due to better stabilization of the leaving chloride anion with the Lewis acid ZnCl<sub>2</sub>. It is shown below that the energy difference of the two activation models is much larger in the reaction of a zinc alkoxide cluster encountered in the SS reaction of an allylic alcohol.

**3. The SS Reaction of Allylic Alcohol.** Experimental studies showed that the SS reaction of allyl alcohol is much faster (>1000 times) than that of a simple olefin.<sup>5</sup> We investigated this phenomenon in several stages: (1) an intramolecular cyclopropanation reaction of monomeric (allyloxy)ZnCH<sub>2</sub>Cl in the absence and the presence of ZnCl<sub>2</sub>, (2) an intramolecular cyclopropanation reaction of dimeric (allyloxy)<sub>2</sub>ZnCH<sub>2</sub>Cl in the absence and the presence of ZnCl<sub>2</sub>, and (3) tetrameric (allyloxy)<sub>4</sub>ZnCH<sub>2</sub>Cl with ZnCl<sub>2</sub>. Recent experimental studies on the structures of halomethylzinc alkoxides by Charette et al. revealed that allyloxylzinc species exist as a monomer in a benzene

(26) Denmark, S. E.; O'Connor, S. P. *J. Org. Chem.* **1997**, *62*, 584–594.  
 (27)  $\Delta H^\ddagger = 17.3$  kcal/mol at 0 K,  $\Delta S^\ddagger = -32.5$  cal/(mol K), and  $\Delta G^\ddagger = 26.2$  kcal/mol at 0 °C, 1 atm. These values are reasonable for a concerted cycloaddition. The kinetic parameters of inter- and intramolecular Diels–Alder reactions: Grimme, W.; Wiechers, G. *Tetrahedron Lett.* **1987**, *28*, 6035–6038.

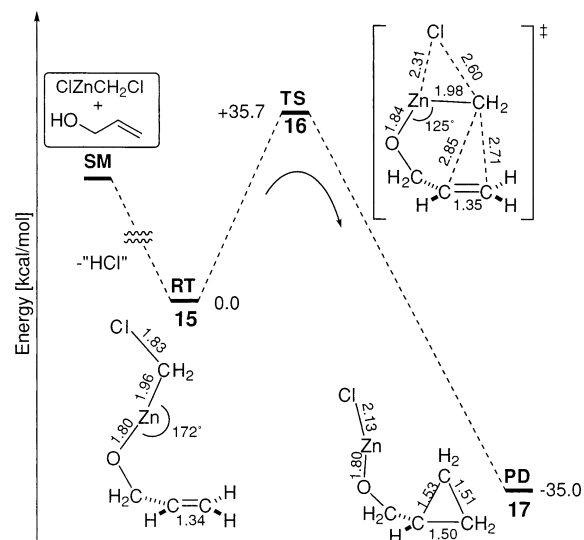


**Figure 5.** Structures and energetics of cyclopropanation of allyl alcohol with  $\text{ClZnCH}_2\text{Cl}$  via a monomeric alkoxy complex (B3LYP/631A level). Bond lengths are shown in angstroms. Energies relative to **15** are shown in kilocalories per mole.

solution and a tetramer in the solid phase.<sup>28</sup> The present step-by-step approach therefore provides useful information on the actual events in the reaction mixture, where the monomeric pathway and aggregation can compete with each other.

**A. Allyloxy Zinc Monomer and Its  $\text{ZnCl}_2$  Complex.** We examined first the monomeric reaction pathway of the cyclopropanation of allyl alcohol, as shown in Figure 5. It is known experimentally that the SS cyclopropanation of a free allylic alcohol takes place through initial formation of an allylic alkoxy.<sup>29</sup> The product, cyclopropylmethoxide **17**, forms from **15** through the transition state of the cyclopropanation of **16**. The calculated activation energy is 35.7 kcal/mol and is far higher than the energy expected from the experimental conditions (0 °C in  $\text{CH}_2\text{Cl}_2$ ). The forming C–C bonds in TS **16** are longer than those of the cyclopropanation of ethylene (2.4 and 2.6 Å, respectively), suggesting that TS **16** is earlier than the TS of the latter case. The angle O–Zn–C in **15** is 172°, and the corresponding angle in **16** is 125°. One can speculate that such a large structural change causes a large deformation energy and raises the activation energy. We therefore calculated hypothetical bent structures of  $\text{CH}_3\text{ZnOH}$  of  $C_s$  symmetry (see ref 30). The decrease of the bond angles  $\theta$  from 172° to 125° resulted in destabilization of the molecule by as much as 13.8 kcal/mol.

We also examined the SS reaction of ethylene with chloromethylzinc methoxide (**18**) to evaluate electronic effects of the

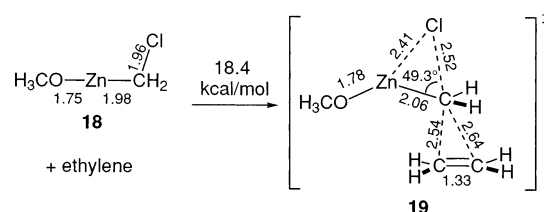


**Figure 6.** Cyclopropanation of ethylene with chloromethylzinc methoxide (**18**) at the B3LYP/631A level.

alkoxy group (Figure 6, at the B3LYP/631A level). While the SS reaction with halomethylzinc alkoxy (not allyloxy) has proved not to be an experimentally feasible reaction, the activation energy was found to be 18.4 kcal/mol, which is only 1.1 kcal/mol higher than that of  $\text{ClZnCH}_2\text{Cl}$  (**7**) (in Figure 2).<sup>29,31</sup> The above results show that the high activation energy with **16** is due to bending of the linear O–Zn–C bond in the TS (**16**) of the reaction of allyloxy zinc complex **15** rather than due to the electronic effect of the allyloxy group.

Given the unrealistically high activation energy in the monomeric reaction pathway, we studied the effect of a Lewis acid (Figure 7, modes 1 and 2). Coordination of  $\text{ZnCl}_2$  to the oxygen atom of allyl alcohol resulted in the formation of **20**, which possesses a four-centered dinuclear zinc complex structure. Such structures have been frequently suggested as reactive species, as shown in Scheme 3. The activation energy remained very high (29.4 vs 35.7 kcal/mol in Figure 5). The angle C–Zn–O in the starting material **20** decreased to 149°, and thus a part of the energetic cost of C–Zn–O bending in the TS is paid already at the starting stage.

The mode 2 pathway with allyl alcohol was also studied, and the results are shown on the right-hand side of Figure 7. The mode 2 activation is much more effective than mode 1 as to the C–C bond formation, but overall energetic loss against the latter is evident. The much lower affinity of  $\text{ZnCl}_2$  for a chlorine atom than for an oxygen atom resulted in the large energy loss in mode 2 against mode 1.

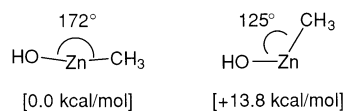
The properties of reactants, complexes, and TSs may differ considerably between the gas phase and the solution phase. Two types of effects of the solvent on the reaction pathway were examined, the bulk polarity and the explicit solvent coordination for the conversion of **20** to **22**. When the dipole moment of  $\text{CH}_2\text{Cl}_2$  (a solvent frequently used in the SS reaction; dielectric constant,  $\epsilon = 9.814$  at 0 °C) is considered with the SCRf method<sup>22</sup> (without structure optimization), the activation energy decreased by 1.5 kcal/mol to 26.4 kcal/mol. This reduction of the activation energy may be due to stabilization of the polarization of the C<sup>1</sup>–Cl bond. Explicit solvent coordination was investigated next.

When a Lewis base solvent, dimethyl ether, was allowed to coordinate to  $\text{Zn}^1$  in **20**, the activation energy (from **20a** to **22a**) increased by 6 kcal/mol (Figure 8). When a chloromethane molecule was allowed to coordinate to the same  $\text{Zn}^1$  atom as in **20b**, the activation energy (from **20b** to **22b**) decreased by 1.1

(28) Charette, A. B.; Molinaro, C.; Brochu, C. *J. Am. Chem. Soc.* **2001**, *123*, 12160–12167. Although the authors did not observe aggregates of halomethylzinc alkoxy in a benzene solution, the participation of an aggregate species in the SS reaction cannot be excluded, as pointed out by the authors.

(29) Charette, A. B.; Brochu, C. *J. Am. Chem. Soc.* **1995**, *117*, 11367–11368. Halomethylzinc aryloxy and halomethylzinc triflate, which contain less coordinative ligands than an alkoxy ligand, are more effective cyclopropanating reagents than the conventional halomethylzinc halides. Yang, Z. Q.; Lorenz, J. C.; Shi, T. *Tetrahedron Lett.* **1998**, *39*, 8621–8624. Charette, A. B.; Francoeur, S.; Martel, J.; Wilb, N. *Angew. Chem., Int. Ed.* **2000**, *39*, 4539–4542.

(30) Bent structures of  $\text{CH}_3\text{ZnOH}$  (B3LYP/631A level).



(31) Although the theoretical activation energy of ca. 18 kcal/mol predicts the cyclopropanation reaction of halomethylzinc alkoxy to be as feasible as that of halomethylzinc halide, the former reaction is very sluggish at ambient temperature without activation by a Lewis acid.<sup>28</sup> This inconsistency in the experimental observation and the theoretical activation energy can be explained by considering the generation of higher aggregates of zinc species, in which the zinc atom of the carbenoid is coordinatively saturated, as shown in the following sections.

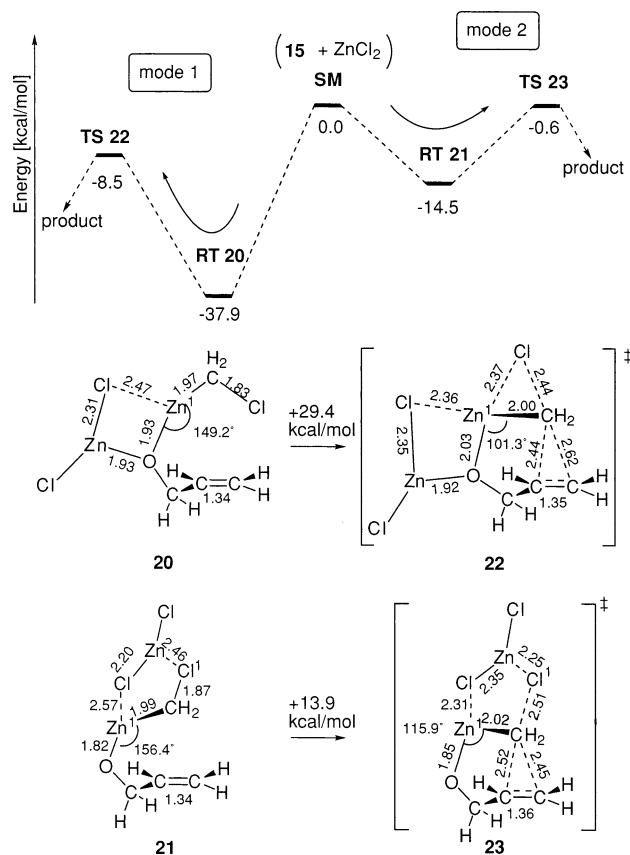


**Figure 7.** Energy profile of cyclopropanation of allyloxide monomer with  $\text{ClZnCH}_2\text{Cl}$  in the presence of  $\text{ZnCl}_2$  (B3LYP/631A level). Mode 1: coordination of  $\text{ZnCl}_2$  to oxygen. Mode 2: coordination of  $\text{ZnCl}_2$  to  $\text{Cl}^1$ . Bond lengths are shown in angstroms. Energies relative to the starting materials are shown in kilocalories per mole.

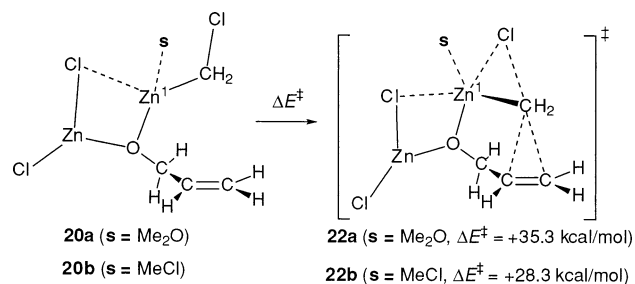


**Figure 8.** Solvation model of the cyclopropanation of allyloxide monomer with  $\text{ClZnCH}_2\text{Cl}$  (B3LYP/631A level). (a)  $\text{Me}_2\text{O}$  coordination to Zn atom ( $\text{Zn}^1$ ) of the SS reagent and (b)  $\text{MeCl}$  coordination to the same Zn atom.

kcal/mol to 28.3 kcal/mol. The Lewis base solvent attenuates the Lewis acidity of the zinc atom and slows down the SS reaction.

**B. Allyloxzinc Dimer and Its  $\text{ZnCl}_2$  Complex.** Zinc alkoxides (e.g., **15** and **18**) form higher aggregates in the solid phase,<sup>28,32</sup> and such aggregates are considered a necessary intermediate of ligand exchange processes in Schlenk-type equilibria of organozinc reagents. We thus investigated the reaction of the aggregate starting with dimer models. The di- $\mu$ -oxo bridged species **24** in Figure 9 is a model dimer and undergoes an intramolecular cyclopropanation with a 28.0 kcal/mol activation energy (**25**). This result indicates that such a higher aggregate itself is unlikely as a reactive intermediate of

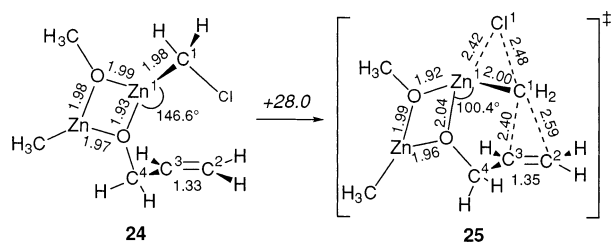


**Figure 9.** Cyclopropanation of allyloxide dimer with  $\text{ClZnCH}_2\text{Cl}$  (B3LYP/631A level). Bond lengths are shown in angstroms. Energies relative to **24** are shown in italics.

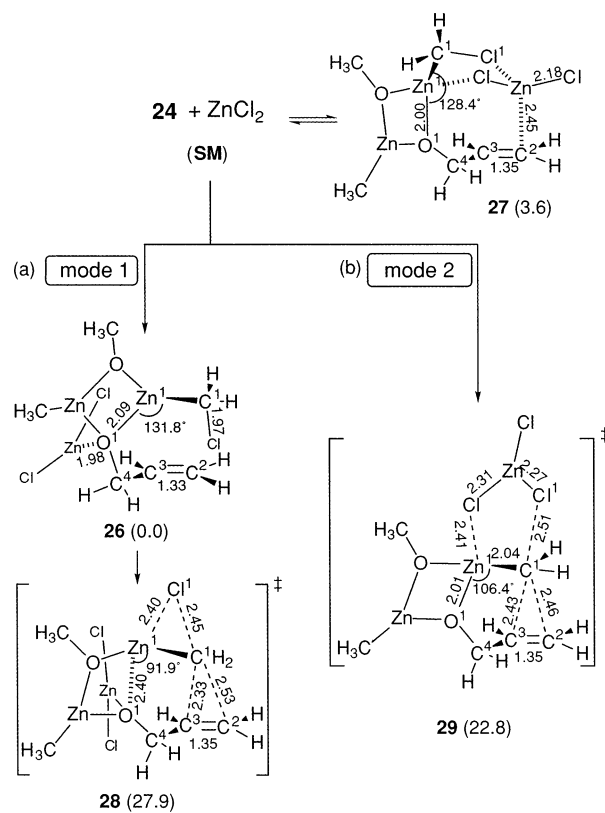


**Figure 10.** Lewis acid activation model of cyclopropanation of allyloxide dimer with  $\text{ClZnCH}_2\text{Cl}$  (B3LYP/631A level). (a) Mode 1,  $\text{ZnCl}_2$  coordination to  $\text{O}^1$ , and (b) mode 2, to  $\text{Cl}^1$ . Bond lengths are shown in angstroms. Energies relative to **26** are shown in parentheses.

the SS reaction, in agreement with the experimental observations.<sup>28</sup>

Coordination of a Lewis acid such as  $\text{ZnCl}_2$  to the chlorine atom of the SS reagent is found to reduce the activation energy in the dimer model. The  $\text{ZnCl}_2$  complexes **26** and **27** in Figure 10 are the dimer models of mode 1 and mode 2 activation, respectively. The effect of mode 1 activation with  $\text{ZnCl}_2$  (**26** to **28**) was found to be negligible ( $\Delta E^\ddagger = 27.9$  kcal/mol; Figure 10, mode 1).  $\text{Zn}^1$  lies far (2.40 Å) from the oxygen atom in **28**, and there is no true coordination between the two atoms, because the  $\text{O}^1$  atom is tricoordinated in **26** and hence no longer a Lewis base.

In sharp contrast to the negligible effect of the mode 1 activation on the activation energy of the cyclopropanation, mode 2 activation on **24** (Figures 10 and 11, mode 2) was found to lower the barrier height to ca. 13 kcal/mol. Unlike the  $\text{O}^1$  atom, the  $\text{Cl}^1$  atom is not involved in the aggregate, and therefore coordination of  $\text{ZnCl}_2$  to the  $\text{Cl}^1$  group takes place easily. In these gas-phase calculations, we located a nonproductive

(32) Shearer, H. M. M.; Spencer, C. B. *Acta Crystallogr., Sect. B* **1980**, *36*, 2046–2050.

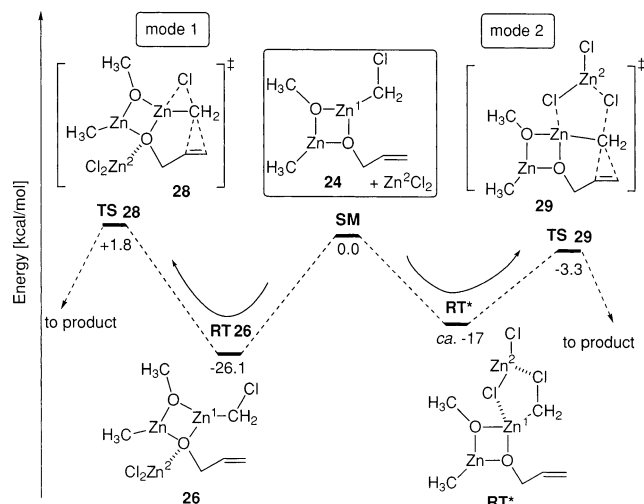


**Figure 11.** Energy profile of Lewis acid activation model of cyclopropanation of allyloxide dimer with  $\text{ClZnCH}_2\text{Cl}$  (B3LYP/631A level). Energies relative to the starting materials are shown in kilocalories per mole.  $\text{RT}^*$ , representing an intermediate of the mode 2 pathway, was optimized with restriction of the dihedral angle  $\text{Zn}^1\text{-CH}_2\text{-Cl-Zn}^2$  to avoid an artifact of the gas-phase calculation, that is, the interaction between the  $\text{C}=\text{C}$   $\pi$  bond and  $\text{Zn}^2$  (found in the nonproductive intermediate **27**).

intermediate **27**, where the added zinc chloride is held among  $\text{Zn}^1$ ,  $\text{Cl}^1$ , and the olefin. The TS of the cyclopropane formation (**29**) was located 19.1 kcal/mol above **27**. Even considering the 3.6 kcal/mol energy difference between **26** and **27** (Figure 11), mode 2 activation is favored over mode 1 activation by 5.1 kcal/mol (**29** – **28**) in terms of the barrier height of the methylene transfer. The trimetallic TS **29** involves a rigid polycyclic framework. The dihedral angle  $\text{C}^2\text{-C}^3\text{-C}^4\text{-O}$  in **29** was found to be  $132^\circ$  and agrees with the value experimentally suggested in Denmark's asymmetric SS reaction (ca.  $150^\circ$ ).<sup>26</sup>

**C. Allyloxyzinc Tetramer and Its  $\text{ZnCl}_2$  Complex.** In the solid state,  $\text{CH}_3\text{OZnCH}_3$  exists as a cubic tetramer<sup>32</sup> and may also do so in a weakly coordinative solvent. We therefore investigated the effect of  $\text{ZnCl}_2$  complexation on the reaction of a tetrameric complex of the allyloxy-type SS reagent. Because of the large size of the calculations, we performed the calculations here at the level of B3LYP/631A/HF/321A. The optimized structures are shown in Figure 12. In **30a**, where, in the initial geometry, we put  $\text{ZnCl}_2$  closer to the oxygen atom of the allyl alkoxide (i.e., mode 1), the  $\text{O}^1\text{-Zn}^1$  distance became 4.03 Å after geometry optimization. The alkoxide oxygen,  $\text{O}^1$ , coordinates to three zinc atoms so that it is no longer a sufficiently strong Lewis base to accept  $\text{ZnCl}_2$ . In **30b** (mode 2),  $\text{ZnCl}_2$  is attached to the chlorine atom  $\text{Cl}^1$  ( $\text{Zn}\text{-Cl}^1$ : 2.49 Å). Because of this coordination, **30b** is 5.1 kcal/mol more stable than **30a**. From **30b**, we obtained the TS of cyclopropanation **31** with mode 2 activation, which lies 12.9 kcal/mol above **30b**, whereas a TS with mode 1 activation could not be obtained (because of the lack of Lewis acidity of the  $\text{Zn}^2$  atom).

In both the dimeric and the tetrameric models, the allyloxy oxygen atoms in the aggregates are no longer basic and hence are unlikely to serve as an anchor to a Lewis acid. On the other hand, the efficiency of the Lewis acid activation of the halide group on the carbenoid carbon atom is not affected by the aggregation state of the zinc allyloxy moiety. Charette's recent studies have shown that monomeric halomethylzinc alkoxide (e.g., **15**) is the only experimentally observable dominant species in benzene solution,<sup>28</sup> and the present study suggests that such

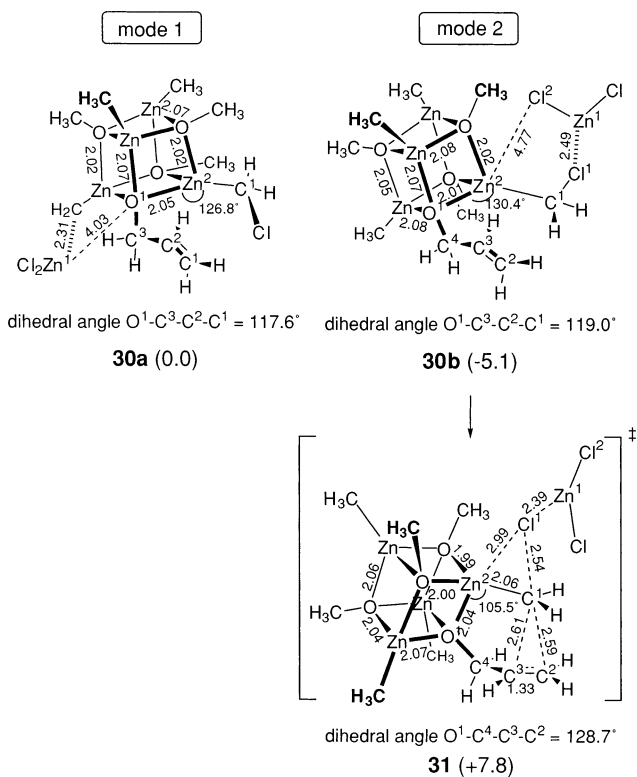


**Figure 12.** Modes 1 and 2 activation models of the tetrameric cluster (B3LYP/631A/HF/321A).

a monomeric species may remain quite unreactive even in the presence of one molecule of a Lewis acid. Therefore, some kind of multimetallic aggregate involving the allyloxyzinc SS reagent is likely to be a reactive intermediate.

**D. The SS Reaction with 2-Cyclohexen-1-ol.** The hydroxy-group-directed SS reaction of 2-cyclohexen-1-ol is a pioneering example of a functional-group directed stereoselective reaction.<sup>32</sup> The kinetic effect as shown in Scheme 1 is rather subtle (i.e., a rate constant difference of only 3.35 times); nonetheless, we examined this case because of its historical and practical importance. Two conformers of cyclohexenols, *O*-pseudoequatorial and *O*-pseudoaxial 2-cyclohexen-1-ols, were used as models of *cis*- and *trans*-5-methyl-2-cyclohexen-1-ols. The methyl group, which occupies the equatorial position in each half-chair conformer of the cyclohexenol, was omitted for simplicity.

The model pathway for the pseudoequatorial cyclohexenol is shown on the right-hand side of Figure 13 (at the B3LYP/631A/B3LYP/321A level). Two complex structures, **32** and **33**, were found. Whereas **33** is a nonproductive complex, **32** goes smoothly to the TS of cyclopropanation **34**. The TS **34** for pseudoequatorial cyclohexenol is similar to that for the allylic alcohol (e.g., as to the two forming  $\text{C-C}$  bonds, 2.59 and 2.42 Å, and the angle  $\text{C}^1\text{-C}^2\text{-C}^3$ ,  $67.2^\circ$ ). The dihedral angle  $\text{O-C}^4\text{-C}^3\text{-C}^2$  is  $140.0^\circ$  and again is in good agreement with Denmark's suggestion.<sup>26</sup>

The reaction pathway of the cyclopropanation with pseudoaxial cyclohexenol is shown on the left-hand side of Figure 13. Two complexes (**36** and **37**), transition state **38**, and cyclopropane product **39** were obtained. The energetics of the two pathways are compared. As seen from the energy diagram, the pseudoequatorial pathway is favored by 0.8 kcal/mol over the alternative (calculation at 25 °C to be 80% selective: Curtin–



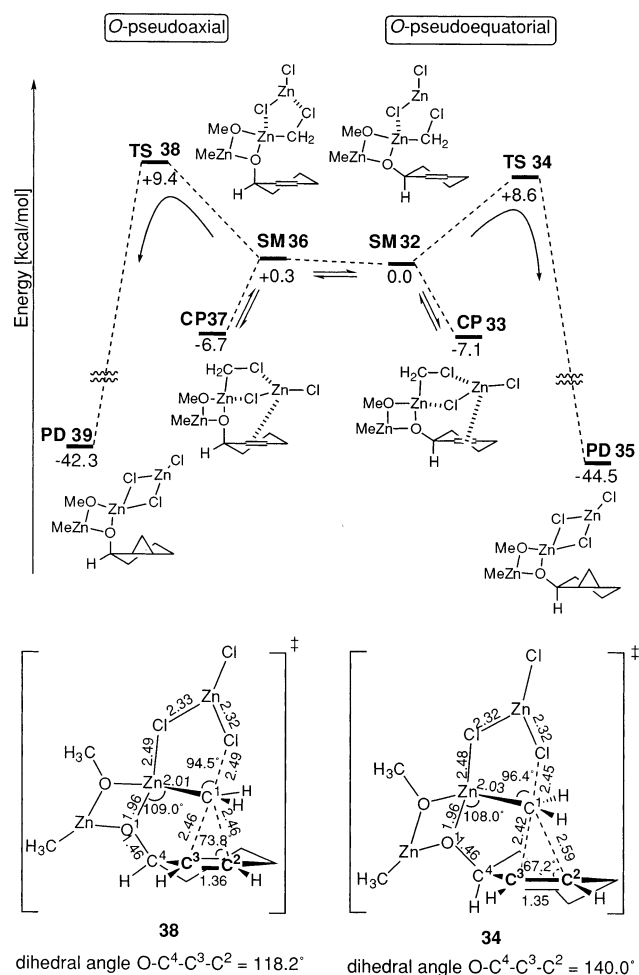


**Figure 13.** Energy profile of the SS reaction with *O*-pseudoaxial and axial cyclohexenol (B3LYP/631A/B3LYP/321A level). Bond lengths are given in angstroms, and relative energies from **32** are given in kilocalories per mole.

Hammett conditions being satisfied). The 0.8 kcal/mol energy difference is perhaps too small to be truly meaningful, yet it is still in accord with the experimental results (experimental relative rate constants of 3.35:1 in Scheme 1 correspond to 0.73 kcal/mol energy difference). As the geometries of the Zn<sub>2</sub>-containing fragment in **34** and **38** are very similar to each other, the major difference between these two TSs resides in the conformation of the cyclohexene moiety.

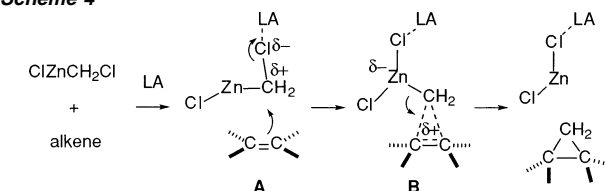
## Conclusion

The present studies revealed that the reaction pathway of cyclopropanation with a metal carbenoid depends on the nature of the metal cation and its aggregation state. With lithium carbenoid, two paths, methylene transfer and carbometalation/elimination reaction pathways, have similar activation energies. On the other hand, the methylene transfer pathway is the favored reaction course in the SS reaction.

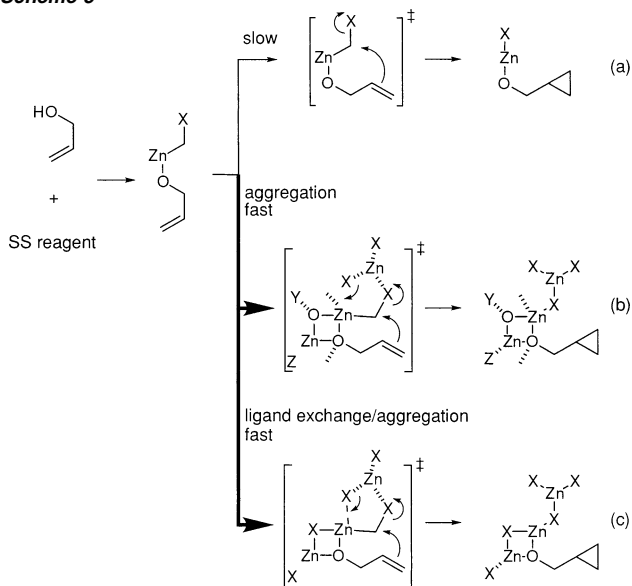
The methylene transfer reaction takes place through two stages: an S<sub>N</sub>2-like displacement of the leaving group by the olefin (**A**), followed by cleavage of the C–Zn bond (**B**) to give the cyclopropane ring. The formalism of the reaction is illustrated in Scheme 4.

The SS reagent reacts much faster with an allylic alcohol than with a simple alkene.<sup>5</sup> It is known that an allyloxy zinc

## Scheme 4



## Scheme 5

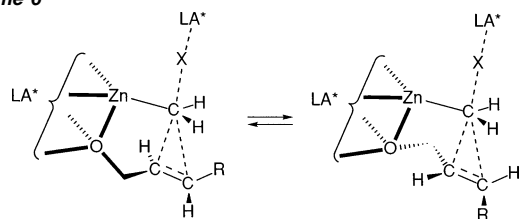


SS reagent forms quickly upon mixing the SS reagent and the allylic alcohol (Scheme 5).<sup>29</sup> Therefore, the faster rate seems to be due to the intramolecular nature of the methylene transfer. As shown above, however, the reality is more complex because the monomeric complex **15** undergoes intramolecular cyclopropanation with an extremely high activation energy (Scheme 5a).

Two events appear to be involved in the cyclopropanation reaction of the allyloxy zinc complex (Scheme 5b): oligomerization of the Zn–O moiety and coordination of the leaving X group by the Lewis acid (ZnX<sub>2</sub>), which can be added on purpose or is generated in situ as a byproduct of the SS reaction. Although a monomeric halomethylzinc alkoxide is a predominant species in solution, ligand-scrambling of halomethylzinc alkoxides suggests the existence of an aggregate as a short-lived intermediate.<sup>28</sup> The Lewis acid coordination to the halogen atom on the halomethyl ligand (–CH<sub>2</sub>X), which has been fully elaborated in the present studies, is likely to be a key event in the SS cyclopropanation reaction. After all of the theoretical and experimental studies, however, the origin of the very fast SS reaction of an allylic alcohol is not entirely clear. In light of the low reactivity of experimentally and theoretically identifiable monomers (Scheme 5a), we suggest two possibilities (Scheme 5b and c). One is the involvement of the allyloxyzinc dimer, which was discussed in the text. A similar but mechanistically different possibility is the involvement of a mixed aggregate of the allyloxyzinc and Lewis acid aggregates, such as (ZnX<sub>2</sub>)<sub>2</sub>.

Our model provides little information on the mechanism of asymmetric cyclopropanation induced by a chiral Lewis acid. On the basis of the present results, however, one can speculate that the enantioselectivity arises from the diastereoisomerism as to the orientation of the allyloxy group relative to the zinc

Scheme 6



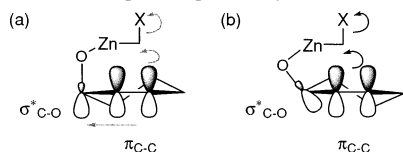
alkoxide cluster containing the chiral Lewis acid (LA\*, Scheme 6). Diastereoselective coordination on the leaving group X can also play some role.

The faster rate of the SS cyclopropanation of 2-cyclohexen-1-ol in an *O*-pseudoequatorial conformation than in an *O*-pseudoaxial one has been the subject of considerable speculation. It was once ascribed to the dimeric transition state shown in Scheme 3a and recently ascribed to the deactivation of the  $\pi_{C-C}$  orbital by interaction with the  $\sigma_{C-O}^*$  orbital, which is absent in the pseudoequatorial conformer.<sup>33–35</sup>

(33) Hoveyda, A. H.; Evans, D. A.; Fu, G. C. *Chem. Rev.* **1993**, *93*, 1307–1370.

(34) The natural population charges (B3LYP/631A//B3LYP/321A level) on C<sup>2</sup> and C<sup>3</sup> in the *O*-pseudoequatorial isomer **32** are +0.004 and –0.026, and those in the *O*-pseudoaxial isomer **36** are –0.002 and –0.024, respectively.

(35) Overlap of the  $\pi_{C-C}$  orbital and the  $\sigma_{C-O}^*$  orbital (a) in *O*-pseudoaxial cyclohexenol and (b) in *O*-pseudoequatorial cyclohexenol. See also ref 33.



The present calculations predict that the pseudoequatorial isomer reacts 4 times faster than the pseudoaxial one. The estimated rate difference is close to the experimental value of 3.35, which is rather too small to discuss in detail. Nonetheless, our model supports the argument in ref 35; that is, the electron-withdrawing C–O bond retards the reaction in this conformation, because the SS reaction is essentially a nucleophilic substitution of the X leaving group on the zinc carbenoid by the olefin. We expect that the models that we have proposed will be useful for the design of new SS reagents to achieve higher selectivity and new reactivity.<sup>36</sup>

**Acknowledgment.** This work was supported by a Grant-in-Aid for Scientific Research (Specially Promoted Research) and a Grant-in-Aid for Young Scientists (A) from the Ministry of Education, Culture, Sports, Science and Technology (Mombukagakusho). This study was also supported by a Grant-in-aid for The 21st Century COE Program for Frontiers in Fundamental Chemistry from Mombukagakusho. A generous allotment of computational time from the Institute for Molecular Science, Okazaki, Japan, and from the Intelligent Modeling Laboratory, The University of Tokyo, is gratefully acknowledged.

**Supporting Information Available:** Cartesian coordinates and total energies at each level of theory for the optimized stationary points (PDF). This material is available free of charge via the Internet at <http://pubs.acs.org>.

JA026709I

(36) Charette, A. B.; Beauchemin, A.; Francoeur, S. *J. Am. Chem. Soc.* **2001**, *123*, 8139–8140.